

## Rubber-based acrylate resins: An alternative for tire recycling and carbon neutral thermoset materials design

Thi Kieu Nhung Tran,<sup>1</sup> Gaël Colomines,<sup>1</sup> Eric Leroy,<sup>2</sup> Arnaud Nourry,<sup>3</sup> Jean-François Pilard,<sup>3</sup> Rémi Deterre<sup>1</sup>

<sup>1</sup>LUNAM Université, IUT de Nantes, CNRS, GEPEA, UMR 6144, OPERP, 2 Avenue du professeur Jean ROUXEL, BP 539, Carquefou 44475, France

<sup>2</sup>LUNAM Université, CNRS, GEPEA, UMR 6144, CRTT, 37, Boulevard de l'Université, St Nazaire Cedex 44606, France

<sup>3</sup>LUNAM Université, Université du Maine, UMR CNRS 6283, Institut des Molécules et Matériaux du Mans, Avenue Olivier Messiaen, Le Mans Cedex 9 72085, France

Correspondence to: G. Colomines (E-mail: gael.colomines@univ-nantes.fr)

**ABSTRACT:** Rubber is a widely available potential carbon neutral resource, both as native natural rubber state and as vulcanized state in waste tires. Herein, we describe a model synthesis of acrylate telechelic natural rubber (AcTNR) oligomers and the use of such oligomers to prepare novel acrylate resins. AcTNR oligomers are synthesized according to a two steps procedure implying a controlled C = C bond's scission of high-molecular-weight natural rubber and a further chain ends functionalization. The molar mass of the resulting AcTNR is found to be 2300 g/mol as determined by <sup>1</sup>H NMR. AcTNR-based resins are then prepared by mixing AcTNR oligomers with various reactive diluents (RD) such as styrene, 1,4-butanediol ether, tri(propylene glycol) diacrylate, 1,6-hexanediol diacrylate, trimethylolpropane triacrylate (AcTNR:RD weight ratio 7:3). These bio-based resins are afterward cured in the presence of methyl ethyl ketone peroxide as initiator and cobalt octoate as accelerator at 80 °C and postcured at 120 °C. The cured resins offer a wide range of mechanical, thermal, and dynamic-mechanical performances. This approach could be extended to rubber tire wastes.

© 2016 Wiley Periodicals, Inc. *J. Appl. Polym. Sci.* **2016**, *133*, 43548.

**KEYWORDS:** crosslinking; monomers; oligomers and telechelics; resins; rubber

Received 9 November 2015; accepted 16 February 2016

DOI: 10.1002/app.43548

### INTRODUCTION

In this “Plastic Age”, the transition from petroleum-based to carbon neutral polymers is a serious concern. Beside the design of bio-based plastics directly from biomass, the efficient recycling of end-life materials is a potentially more important issue.<sup>1–4</sup> This is particularly true for rubber. Natural rubber (NR) is an annually renewable feedstock available in large quantities from rubber trees, mostly *Hevea brasiliensis*. Thanks to its remarkably elastic property, NR, as Suzuki pointed out, has eventually led to a multi-billion dollar industry, and affected the vast majority of people live on this planet.<sup>5</sup> Before World War II, NR accounted for practically 100% of all rubber usage, two-thirds of this total usage was for tires.<sup>6</sup> NR has exceptionally well survived despite the onslaught of synthetic rubbers, and today still represents nearly one-third of all rubber in the marketplace. Concurrently, limited research efforts have been dedicated to the direct use of un-vulcanized NR as a raw biomass

resource for the design of novel bio-based polymeric materials.<sup>7–10</sup> Such materials are based on “telechelic” liquid NR, defined as a low molecular weight NR of 10<sup>3</sup>–10<sup>4</sup> g/mol, approximately, and bearing terminal groups capable of being used in further chain extension and crosslinking.<sup>11</sup> The novel bio-based polymers are mostly hydroxy-telechelic NR-based Polyurethanes with final aspects such as elastomers,<sup>7,12</sup> foams,<sup>9</sup> interpenetrating polymer network (IPN),<sup>13</sup> block copolymers.<sup>14</sup>

Another important issue addressed to rubber industry is the recycling of rubber at vulcanized state since the European Commission has banned the stockpile of waste tires as landfill<sup>15</sup> in a Directive published in 1999. Actually, the worn tires are burnt in cement kilns<sup>16</sup> or electricity generation plants,<sup>17</sup> but with a minor consummation comparing to billion tons of waste tire thrown out every year.<sup>18</sup> As consequence, the reclaiming of waste tire is the most desirable approach in order to solve the disposal problem and also to save precious fossil resources. The

Additional Supporting Information may be found in the online version of this article.

© 2016 Wiley Periodicals, Inc.

reclaiming of waste tires can be categorized in two groups: physical reclaiming processes<sup>19–21</sup> and chemical reclaiming processes<sup>22,23</sup> aiming to devulcanize the cross-linking network of rubber.

A promising chemical reclaiming approach is to produce oligomers by polyisoprene/polybutadiene main-chain scission reactions using inorganic compounds. The first attempts reported required high temperatures<sup>24</sup> or did not allow controlling the molecular weight or the functionality of the smaller molecules obtained.<sup>23</sup> More recently, Sadaka *et al.* reported a controlled degradation of waste tires by an oxidative cleavage with periodic acid at low temperature (30 °C) in order to generate telechelic carbonyl oligomers.<sup>25</sup> Interestingly, such oligomers were further chemically modified at both chain ends as illustrated by recent developments in which the carbonyl oligomers were transformed into hydroxyl oligomers used as polyols for the preparation of polyurethane foams.<sup>9,26</sup>

In the present work, we show the above described functional rubber oligomer synthesis applied to NR. Acrylate telechelic NR (AcTNR) oligomers were synthesized as a model product, which was then used for the formulation of a variety of bio-based thermoset resins. The thermal, dynamic-mechanical, mechanical properties of the cured resins were also discussed.

## EXPERIMENTAL

### Materials

Styrene (STY), 1,4-butanediol ether, tri(propylene glycol) diacrylate (TPGDA), 1,6-hexanediol diacrylate (HDDA), trimethylolpropane triacrylate (TMPTA), methyl ethyl ketone peroxide (MEKP), were purchased from Sigma-Aldrich and used without any further purification. NR (NR) was 10 CV 60 from Hutchinson. Tetrahydrofuran (THF), Dichloromethane (DCM), Sodium chloride (NaCl), Sodium bicarbonate (NaHCO<sub>3</sub>), Sodium thiosulfate (Na<sub>2</sub>S<sub>2</sub>O<sub>3</sub>), Magnesium sulfate (MgSO<sub>4</sub>) were purchased from Fisher and used as received. Cobalt octoate (trade name: COB 6), vinyl ester resin (trade name: HYDREX<sup>®</sup> LS 33390-10) were supplied by SF Composites.

### Methods

**<sup>1</sup>H-NMR Analysis.** <sup>1</sup>H spectra were recorded on a Bruker 400 Fourier transform spectrometer at 400.13 MHz. Chemical shifts are reported in part per million (ppm) downfield from the singlet peak of tetramethylsilane (TMS) using as internal reference. CDCl<sub>3</sub> was used as solvent.

**Ft-IR.** Fourier transform infra-red spectra were recorded using a Nicolet avatar 370 DTGS spectrometer in ATR mode.

**Size Exclusion Chromatography.** The number-average molecular weight and the molar mass dispersity ( $\mathcal{D}_M$ ) were measured at 35 °C on a ThermoFinnigan Size Exclusion Chromatography (SEC) instrument (equipped with a SpectraSYSTEM AS1000 autosampler, a SpectraSYSTEM RI150 detector), using a polymer laboratories (PL) gel 5 mm MIXED-D columns, calibrated with a series of standard polystyrenes (580–483 × 10<sup>3</sup> g mol<sup>-1</sup>). THF (1.0 mL min<sup>-1</sup>) was used as eluent. The concentration of polymeric solutions was 5 mg mL<sup>-1</sup>.

**Differential Scanning Calorimetry.** Differential scanning calorimetry (DSC) analysis was performed on a METTLER TOLEDO (DSC 1) with a heating rate of 20 °C min<sup>-1</sup> in a range of -80 °C to 170 °C, under nitrogen atmosphere. The samples (2–4 mg) were scanned twice. The glass transition temperature ( $T_g$ ) was determined on the onset temperature of transition curve of the first scan. The second scan is for ensuring a reproducible result. Calibration was achieved by using indium as reference material.

**Dynamic Mechanical Thermal Analysis.** Storage modulus ( $E'$ ), loss modulus ( $E''$ ), and loss tangent ( $\tan \delta$ ) were recorded on Q500 (TA Instrument) in tension mode at a frequency of 1 Hz and a deformation of 0.1% on rectangular parallelepiped samples (30 × 8 × 1 mm). Measurements were carried out in the range of -80 °C to 170 °C at a rate of 5 °C min<sup>-1</sup>. Three measurements were done for each sample.  $T_x$  was determined based on the onset temperature of  $E'$ ,  $E''$  peak, and  $\tan \delta$  peak.

**Tensile Testing.** The tensile testing was carried out in Z1010 tester (Zwick/Roell). The samples (ASTM D638 Type IV) were analyzed at a speed of 5 mm min<sup>-1</sup> at room temperature. Three measurements were performed for each sample.

**Viscosity Measurement.** The viscosity of oligomers and resins was measured on HAAKE MARS III rheometer (plate-plate geometry, Ø20 mm) with rotation mode (shear rate of 0.1–1000 s<sup>-1</sup>) at 25 °C. The viscosity's values were evaluated at Newtonian plateau (shear rate < 100 s<sup>-1</sup>).

**Synthesis of Carbonyl-Telechelic NR.** NR block was cut into small pieces (163.12 g, 2.39 mol of repeating unit). These pieces were dissolved in THF (3.5 L) in a jacketed reaction flask (5 L) equipped with a mechanical stirrer, for one night, at room temperature. A solution of periodic acid (H<sub>5</sub>IO<sub>6</sub>) (55.76 g, 0.2446 mol) in THF (0.4 mol/L, 611 mL) was added dropwise into the NR solution. Afterward, the reaction solution was vigorously stirred for 24 h at 30 °C. At the end of the reaction, the solution was filtered and then evaporated. The resulting product was then dissolved in CH<sub>2</sub>Cl<sub>2</sub> (2 L). This solution was washed once with a saturated NaHCO<sub>3</sub> solution (2 L), then once with Na<sub>2</sub>S<sub>2</sub>O<sub>3</sub> solution (20wt %, 2 L), and finally once with saturated NaCl solution (2 L). Then, the organic layer was dried over MgSO<sub>4</sub> overnight. A yellowish viscous liquid was obtained after salt filtration and solvent evaporation (Yield: 85–90%).  $\overline{M}_{n,NMR}=2300$  g/mol,  $\overline{M}_{n,SEC}=4600$  g/mol.

<sup>1</sup>H NMR (400 MHz, CDCl<sub>3</sub>,  $\delta$ ): 9.77(s, 1H, CH<sub>2</sub>CHO), 5.10(s, 1 nH, C = CH), 2.49(m, 2H, CH<sub>2</sub>CHO), 2.43(t, 2H, CH<sub>3</sub>COCH<sub>2</sub>CH<sub>2</sub>), 2.34(m, 2H, CH<sub>2</sub>CH<sub>2</sub>CHO), 2.25(m, 2H, CH<sub>3</sub>COCH<sub>2</sub>CH<sub>2</sub>), 2.13(s, 3H, CH<sub>3</sub>COCH<sub>2</sub>), 2.05(s, nH, CH<sub>2</sub>CCH<sub>3</sub>CHCH<sub>2</sub>), 1.65(s, nH, CH<sub>2</sub>CCH<sub>3</sub>CHCH<sub>2</sub>).

**Synthesis of Hydroxyl-Telechelic NR.** CTNR of molecular weight of 2300 g/mol (145 g, 62.04 mmol) was dissolved in THF (2.25 L) in a jacketed reaction flask (5 L). NaBH<sub>4</sub> (15 g, 65.82 mmol) in THF (80 mL) was added dropwise to a jacketed reaction flask. After stirring overnight at 60 °C, the reaction solution was cooled at room temperature, and then hydrolyzed by adding 300 g of ice. This reaction mixture was washed twice with saturated aqueous NaCl solution and dried over MgSO<sub>4</sub> overnight. The final product was obtained after THF

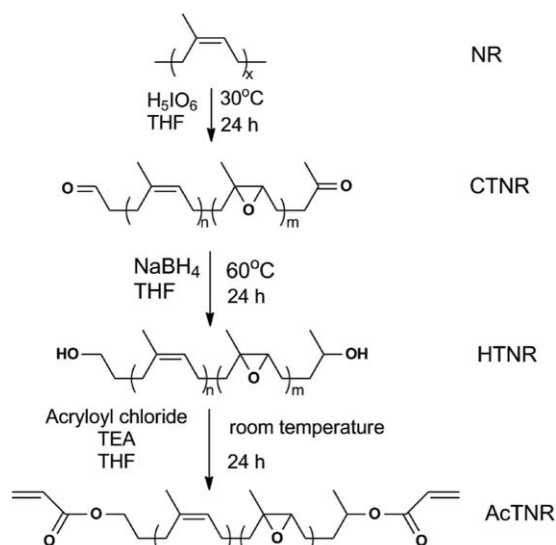


**Figure 1.** Schematic synthetic route of different functionalized-telechelic oligomers derived from NR.

evaporation, as a viscous, yellowish liquid. (Yield: 90–95%).  $\overline{M}_{n,NMR}=2300$  g/mol,  $\overline{M}_{n,SEC}=4300$  g/mol

$^1\text{H NMR}$  (400 MHz,  $\text{CDCl}_3$ ,  $\delta$ ): 5.15(s, 1 nH, C = CH), 3.80(m, 1H, CHOH), 3.65(t, 2H,  $\text{CH}_2\text{OH}$ ), 2.1(s, nH,  $\text{CH}_2\text{CCH}_3\text{CHCH}_2$ ), 1.7(s, nH,  $\text{CH}_2\text{CCH}_3\text{CHCH}_2$ ).

**Synthesis of Acrylate-Telechelic NR.** Acryloyl chloride (10.487 g, 0.1159 mol) in  $\text{CH}_2\text{Cl}_2$  (145 mL) was added dropwise to a

solution containing hydroxy-telechelic NR (HTNR, 97 g, 0.0429 mol), dissolved in 536 mL of anhydrous dichloromethane, and triethylamine (11.726 g, 0.1159 mol), at 0 °C, under argon atmosphere. After maintaining the solution at 0 °C for 30 min, the resulting solution was stirred at room temperature for 24 h. The solution was then transferred in a separating funnel and washed thrice with NaOH aqueous solution (1 N); thrice with HCl aqueous solution (0.5 N); thrice with saturated NaCl solution. The organic layer was dried over  $\text{MgSO}_4$  and filtered. After solvent evaporation, the liquid yellowish oligomer was obtained. Yield (90–95%).  $\overline{M}_{n,NMR}=2400$  g/mol,  $\overline{M}_{n,SEC}=4900$  g/mol.

$^1\text{H NMR}$  (400 MHz,  $\text{CDCl}_3$ ,  $\delta$ ): 6.41 (m, 2H,  $\text{CH}=\text{CH}_2$ ), 6.14 (m, 2H,  $\text{CH}=\text{CH}_2$ ), 5.83(m, 2H,  $\text{CH}=\text{CH}_2$ ), 5.15(s, nH, C = CH), 5.00 (m, 1H, CHOCO), 4.17(t, 2H,  $\text{CH}_2\text{OCO}$ ), 2.1(s, nH,  $\text{CH}_2\text{CCH}_3\text{CHCH}_2$ ), 1.7(s, nH,  $\text{CH}_2\text{CCH}_3\text{CHCH}_2$ ).

**Formulation of Bio-Based Resins.** The resins were prepared by mixing acrylate-telechelic NR (AcTNR) with different reactive diluents belonging to three families: monofunctional (STY; 1,4-butanediol ether), difunctional (TPGDA; HDDA), trifunctional (TMPTA). Five bio-based resins were prepared and listed in Table II. The amount of reactive diluent for all systems was maintained at 30% (wt). These resins were cured by adding MEKP (1 wt %) as initiator and cobalt octoate (0.2 wt %) as accelerator at 80 °C for 15 h and then postcured at 120 °C for 4 h.

## RESULTS AND DISCUSSION

In the present work, NR, a renewable resource, was used as a model compound for the production of acrylate resins. In order to fulfill this goal, three steps of chemical modification of NR

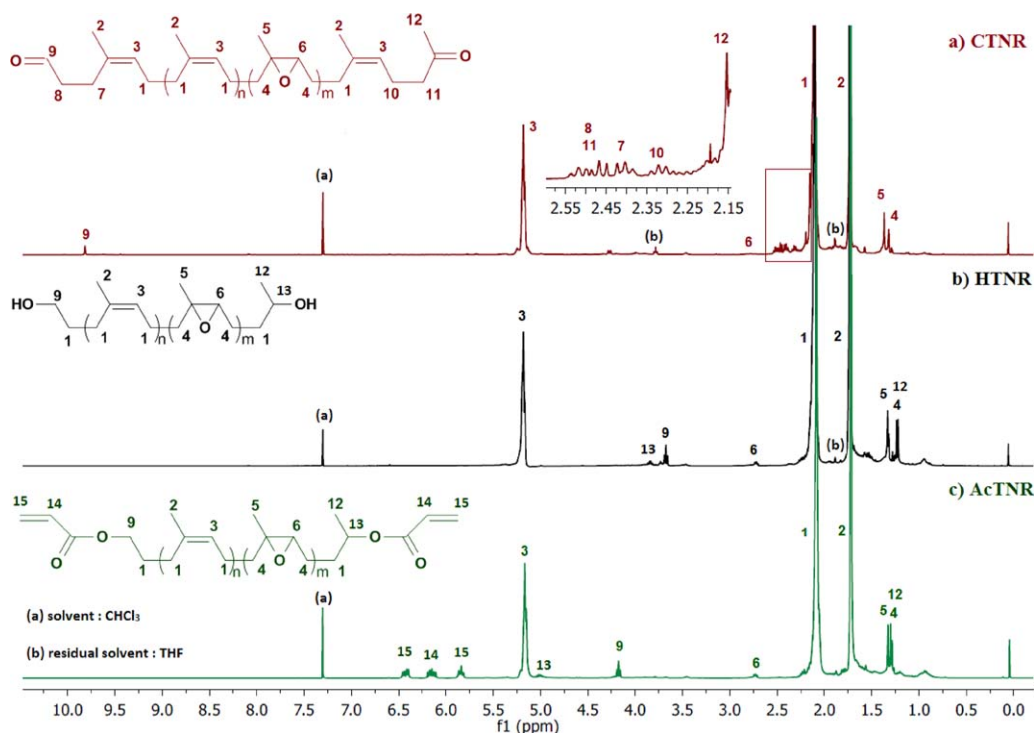


**Figure 2.**  $^1\text{H NMR}$  spectra of (a) CTNR; (b) HTNR; (c) AcTNR (solvent:  $\text{CDCl}_3$ ). [Color figure can be viewed in the online issue, which is available at [wileyonlinelibrary.com](http://wileyonlinelibrary.com).]

**Table I.** The Average Molar Mass and the Molar-Mass Dispersity of Three Oligomers

Oligomers	$\tau_{\text{epoxide}}$ (%)	$\overline{M}_{n,\text{NMR}}$ (g/mol)	$\overline{M}_{n,\text{SEC}}$ (g/mol)	$\mathcal{D}_M$
CTNR	2.0	2300	4600	1.85
HTNR	3.8	2300	4300	1.97
AcTNR	3.7	2400	4900	2.12

were performed. The high molecular weight NR ( $>10^6$  g/mol) was transformed into the carbonyl-telechelic natural rubber (CTNR) with low molecular weight of about 2000 g/mol via an oxidative well-controlled degradation by periodic acid<sup>25</sup>. The two carbonyl groups at the chain ends of these oligomers were then reduced to hydroxyl groups to obtain the hydroxyl-telechelic natural rubber (HTNR) by  $\text{NaBH}_4$ <sup>26</sup>. Afterwards, the HTNR oligomers were converted into the AcTNR via an esterification with acryloyl chloride. Finally, the acrylate resins were produced by mixing the AcTNR oligomers with various reactive diluents categorized into three families: monofunctional such as 1,4-butanediol vinyl ether (BVE); STY; difunctional such as TPGDA; HDDA; trifunctional as TMPTA.

#### Preparation and Characterization of Functionalized-Telechelic Oligomers

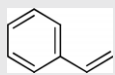
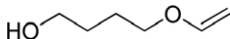
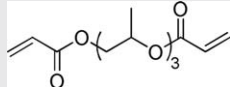
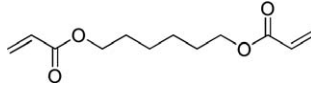
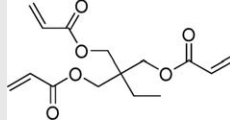
The main component of bio-based resins is an AcTNR; its chemical transformation is shown in Figure 1. The syntheses of these functional oligomers were adapted from previous works in our laboratory.<sup>26,27</sup>

In order to characterize the chemical structure and to determine the molecular weight of the resulting oligomers, spectroscopic and chromatographic methods were employed. The functionality of the synthesized oligomers was checked by  $^1\text{H}$  NMR analysis. The spectrum of CTNR [Figure 2(a)] shows the characteristic signals at 9.8 ppm and at 2.25–2.55 ppm corresponding to aldehyde proton 9 and to methylene protons 7, 8, 10, 11 of chain ends, respectively. These signals were disappeared after the reduc-

tion of carbonyl groups by  $\text{NaBH}_4$  as shown in HTNR's spectrum [Figure 2(b)]. In this spectrum, the new peaks at 3.67 ppm and 3.85 ppm corresponding to the proton 9 attached to primary OH and the proton 13 linked to secondary OH, respectively. After the esterification of HTNR, as shown in Figure 2(c), these protons 9, 13 were shifted to 4.17 ppm and 5.02 ppm, respectively. The new signals of the protons 14, 15 at 5.8–6.4 ppm corresponding to vinyl protons at chain ends were also observed. In addition, we observed the signal at 2.75 ppm representing the proton 6 of epoxidized rubber in three oligomers. The apparition of residual epoxides (2–4%, Table I) was explained elsewhere.<sup>26</sup> Such a small ratio of epoxide would not play an important role for this application on acrylate resin. Moreover, compared to the reported synthesis,<sup>28</sup> such a one-pot method is more favored owing to it being economically viable on an industrial scale, thus it was selected for the preparation of telechelic liquid NR.

The  $^1\text{H}$  NMR spectra were also used to determine the average molar mass ( $\overline{M}_n$ ) of the resulting functional oligomers. The formula for calculating ( $\overline{M}_n$ ) were described elsewhere.<sup>26</sup> The resulting molar masses are listed in Table I. As seen, the functional oligomers of an average molar mass of 2300 g/mol, approximately, were obtained. Furthermore, the number average molecular mass ( $\overline{M}_n$ ) and the molar-mass dispersity ( $\mathcal{D}_M$ ) of the resulting oligomers were determined by size-exclusion chromatography (SEC) with standard polystyrene calibration. The values of ( $\overline{M}_n$ ),  $\mathcal{D}_M$  are summarized in Table I and compared with those determined by  $^1\text{H}$  NMR. The ratio is around 0.5 for three oligomers. This ratio was close to the value found by Busnel *et al.* (0.67).<sup>29</sup> It is known that the molecular mass measured by SEC differs from those determined by NMR. In this SEC equipped with a refractive index detector, the molecular mass was measured by comparing the hydrodynamic volumes of samples to those of polystyrene used as standard. But, the relationship between hydrodynamic volume and the molecular mass is not the same for all polymers, so that the absolute values of ( $\overline{M}_n$ ) cannot be yielded by this SEC equipment.<sup>30</sup>

**Table II.** The Viscosity of Resulting Resins and the Structure of Reactive Diluents Used

Bio-resin <sup>a</sup>	Reactive diluents	Structures of reactive diluents	Viscosity (25 °C, Pa s)
AcTNR-STY	Styrene		0.45 ± 0.01
AcTNR-BVE	1,4-Butanediol vinyl ether		0.52 ± 0.02
AcTNR-TPGDA	Tri(propylene glycol) diacrylate		0.55 ± 0.02
AcTNR-HDDA	1,6-Hexanediol diacrylate		0.38 ± 0.01
AcTNR-TMPTA	Trimethylolpropane triacrylate		3.1 ± 0.4

<sup>a</sup>Bio-resin: ATNR/diluent = 7/3 (wt).

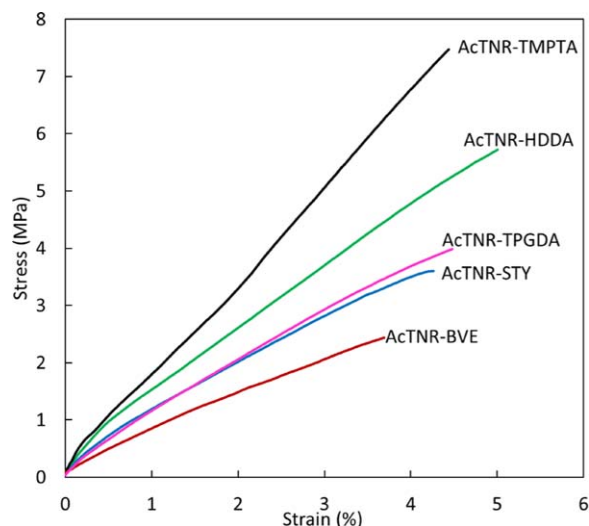


**Figure 3.** Five curves of the tensile test for cured resins. [Color figure can be viewed in the online issue, which is available at [wileyonlinelibrary.com](http://wileyonlinelibrary.com).]

### Resin Formulation and Curing Process

Because of a high viscosity of AcTNR oligomer ( $7.0 \pm 0.1$  Pa s at  $25^\circ\text{C}$ ), it is necessary to mix this oligomer with a reactive diluent in order to obtain a resin with a reasonable viscosity for its later processing. The resins were prepared by mixing the ATNR with three types of reactive diluents: monofunctional (STY, BVE), difunctional (TPGDA, HDDA), and trifunctional (TMPTA). These resins were vigorously stirred for 10 min and stored for two days at room temperature prior to a visual observation of the clarity degree of the mixtures. It was found that the ATNR oligomer had a good miscibility with STY, BVE, TPGDA, HDDA, except TMPTA at weight ratio investigated (30 wt % of diluent). The resins of these diluents (STY, BVE, TPGDA, HDDA) were transparent at room temperature (RT), while those of TMPTA was opaque at RT, but became transparent at  $75^\circ\text{C}$ . Compared to ATNR's viscosity, the viscosity of the resulting resins decreased significantly as summarized in Table II; these low viscous resins might facilitate their processing afterwards.

Among reactive diluents used, STY is the most volatile, so we accept its very small loss during cure process which was chosen inspiring from these processes.<sup>31,32</sup> All bio-based resins were

**Table III.** Tensile Tests of Cured Resins

Bio-resins	Young's modulus (MPa)	Yield stress (MPa)	Yield strain (%)
AcTNR-TMPTA	$177 \pm 14$	$8.0 \pm 0.5$	$4.7 \pm 0.3$
AcTNR-HDDA	$131 \pm 4$	$5.8 \pm 0.1$	$5.1 \pm 0.4$
AcTNR-TPGDA	$105 \pm 4$	$3.8 \pm 0.2$	$4.1 \pm 0.3$
AcTNR-STY	$82 \pm 6$	$2.9 \pm 0.3$	$4.5 \pm 0.3$
AcTNR-BVE	$67 \pm 6$	$2.4 \pm 0.1$	$3.7 \pm 0.1$
Commercial VE	$658 \pm 6$	$47 \pm 3$	$5.7 \pm 0.4$

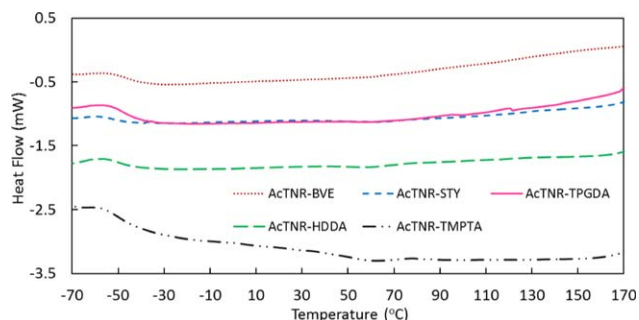


**Figure 4.** Thermograms of five cured resins. [Color figure can be viewed in the online issue, which is available at [wileyonlinelibrary.com](http://wileyonlinelibrary.com).]

cured at  $80^\circ\text{C}$  using MEKP as initiator and cobalt octoate as accelerator, and then postcured at  $120^\circ\text{C}$ . The choice of MEKP/cobalt octoate was inspired from the industrial cure process of vinyl ester resin.<sup>33</sup> The postcure was performed to overcome a possible vitrification which would hinder the diffusion process of reactive molecules.<sup>34</sup>

The FT-IR technique was used to check the curing of five bio-based resins. As shown in Supporting Information (SI), the signal at  $1400\text{ cm}^{-1}$  assigned to vinyl groups of ATNR and reactive diluent are not observable so that we could estimate that the complete curing obtained using the above cure process.

### Characterizations

**Mechanical Behaviors.** The stress-strain plots of cured resins are shown in Figure 3. The curves showed linear deformation behavior with a limited deformation at break (typically 4%). The Young's moduli ( $E$ ) and yield stress values reported in Table III show a strong influence of reactive diluents on the final properties of cured resins. The highest elastic modulus was found in AcTNR-TPMPTA resin (177 MPa) using a trifunctional as reactive diluent. The smallest elastic modulus was observed in AcTNR-STY, AcTNR-BVE resins employing monofunctional diluents. The medium modulus was found for difunctional family with 131 MPa for HDDA and 105 MPa for TPGDA. It was most likely that the stiffness of cured-resins was strongly governed by the density of cross-linked network. Nonetheless, such Young's moduli (67–177 MPa) were low in comparison with those of commercial vinyl ester resin (658 MPa). It was found logical because our resins were based on flexible aliphatic rubber chains while the commercial resins were synthesized from rigid aromatic chains, Bisphenol-A.

**Thermal and Thermal-Mechanical Behaviors.** Differential scanning calorimetry (DSC) and Dynamic Mechanical Thermal Analysis (DMTA) curves obtained for the different cured resins are presented on Figures 4 and 5, respectively. The values of glass transition temperature ( $T_g$ ) determined from DSC and those of  $\alpha$ -relaxation temperature ( $T_\alpha$ ) determined from DMTA curves ( $E'$ ,  $E''$ ,  $\tan \delta$ ) of five cured bio-based resins are listed in Table IV.

As observed in Figure 5(a), storage modulus ( $E'$ ) curves, whatever the nature of reactive diluents, a sharp  $E'$  drop was observed at around  $-43^\circ\text{C}$  attributed to  $T_{\alpha 1}$ . These values of temperature were close to the glass transition temperatures determined by DSC (Table IV) with an average deviation of  $12^\circ\text{C}$  which was not

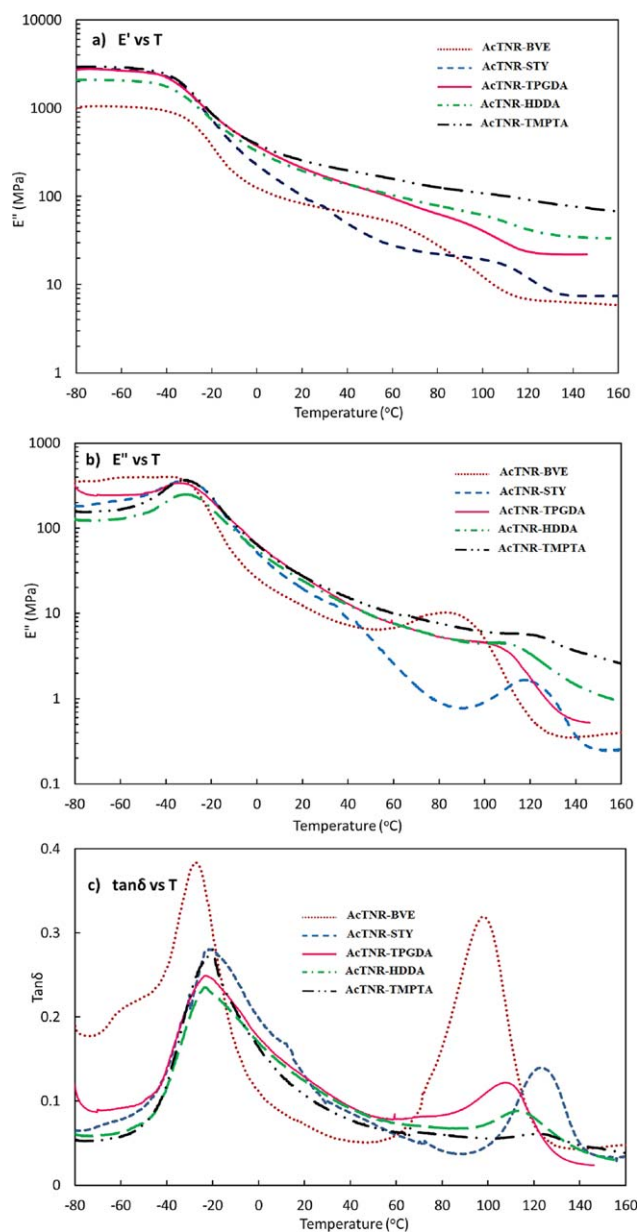


**Figure 5.** DMTA curves of cured resins: (a) storage modulus, (b) loss modulus, and (c)  $\tan \delta$ . [Color figure can be viewed in the online issue, which is available at [wileyonlinelibrary.com](http://wileyonlinelibrary.com).]

surprising since different heating rates were used for the two techniques. While all DSC thermograms show a single heat capacity step revealing a glass transition at  $-55$  °C, approximately (Figure

**Table IV.**  $T_g$  Determined by DSC;  $T_{\alpha}$  Determined from  $E'$ ,  $E''$ ,  $\tan \delta$  of DMTA

Resins	DSC $T_g$ (°C)	$E'$ (DMTA)		$E''$ (DMTA)		$\tan \delta$ (DMTA)	
		$T_{\alpha 1}$ (°C)	$T_{\alpha 2}$ (°C)	$T_{\alpha 1}$ (°C)	$T_{\alpha 2}$ (°C)	$T_{\alpha 1}$ (°C)	$T_{\alpha 2}$ (°C)
AcTNR-BVE	-54	-40	60	-32	87	-27	97
AcTNR-STY	-57	-42	105	-30	120	-22	123
AcTNR-TPGDA	-54	-44	72	-32	110	-23	107
AcTNR-HDDA	-55	-44	102	-31	113	-24	113
AcTNR-TMPTA	-56	-44	-	-30	120	-20	122

4), the respective DMTA evolutions of  $E'$ ,  $E''$ , and  $\tan \delta$  show two thermomechanical transitions (Figure 5). Such evolutions of DMTA curves suggested the presence of two phases in the materials: a soft continuous rubber-rich phase whose glass transition and associated  $\alpha$ -relaxation were detected by both DSC and DMTA; and a rigid dispersed reactive diluent-rich phase acting as a reinforcement of the continuous phase whose  $\alpha$ -relaxation could be only detected by DMTA. The fact that only the second  $\alpha$ -relaxation temperature is influenced by the diluent type, and that its intensity is much lower, supported this assumption. Such a thermomechanical behavior suggested that these materials could be used as damping materials at low temperature (typically down to  $-40$  °C, above the continuous rubber phase glass transition), with adjustable rigidity governed by the reinforcement of reacted diluent-rich phase.

The presence of a phase separation after curing could ascribe to the scarce miscibility of polymer chains of different natures (here the rubber oligomer chains, and the reacted diluent-rich chains). The influence of the reactive diluent on the importance of this phase separation could be evaluated by observing the intensity of  $\tan \delta$  peaks. By assuming that the degree of phase separation of cured resins was related to the sharpness of  $T_{\alpha 2}$ ; the AcTNR-BVE resin had the most significant separation between two phases: rubber-rich phase (ATNR) and diluent-rich phase (BVE). This result was in agreement with the fact that ATNR is hydrophobic while BVE is more hydrophilic. It was not surprising to observe the two  $T_{\alpha}$  in AcTNR-STY resin since the phase separation of polystyrene-*b*-polyisoprene was well-reported in literature.<sup>35</sup> Concerning the difunctional family, the phase separation in AcTNR-HDDA resin was relatively less significant than those of AcTNR-TPGDA resin was. This observation was in accordance with the fact that HDDA is more hydrophobic than TPGDA is; this hydrophobic nature made HDDA more compatible with liquid NR than TPGDA did. In the case of TMPTA resin, a little peak of  $\tan \delta$  suggested a small segregation between rubber phase and diluent phase.

The values of  $E'$  at glassy state ( $-60$  °C) and at rubber state ( $25$  °C) are listed in Table IV. Note that  $E'$  represents the stiffness of viscoelastic material. At lower temperatures, where all phases are in the glassy state, there was no notable difference in terms of the stiffness among trifunctional resin (AcTNR-TMPTA), difunctional resins (AcTNR-TPGDA, AcTNR-HDDA), and monofunctional resin (AcTNR-STY). However, in the case of monofunctional resins, compared to AcTNR-STY, the AcTNR-BVE cured-resin had an exceptionally low stiffness with a storage modulus of 1041 MPa. It was principally because of the difference in chemical structure of

1,4-butanediol ether, flexible aliphatic chain, and STY, rigid aromatic chain. Furthermore, in a plateau-like region (between  $T_{z1}$  and  $T_{z2}$ ), the values of  $E'$  differed from three families of reactive diluents. The small  $E'$  plateau less than 100 MPa for the monofunctional family, the medium  $E'$  plateau around 180 MPa for the difunctional family, the highest  $E'$  plateau about 240 MPa for the trifunctional family were observed. Such results were in accordance with those of Young's moduli from the previous tensile test. These different values of storage modulus were because of the cross-linking network of the cured resins. It is evident that the trifunctional (TMPTA) allowed generating the densest network leading to obtain the highest modulus in the final cured resin.

## CONCLUSIONS

Emerging waste tire recycling strategies based on functional oligomer production by chemical chain scission were adapted to raw NR biomass. A variety of promising low molar mass (around 2300 g/mol) telechelic rubber oligomers (carboxy-telechelic, hydroxyl-telechelic and acrylate-telechelic) were obtained from the native high-molecular-weight NR by a controlled degradation and a functionalization. The AcTNR oligomer was then used as a model product to prepare a series of bio-based thermoset resins. Various reactive diluents categorized in three families were used: monofunctional (BVE, STY), difunctional (TPGDA, HDDA), and trifunctional (TMPTA). Multiphase materials after curing with a rubber-rich continuous phase, reinforced by reactive diluent-rich dispersed phases, were yielded. The thermo-mechanical performances were shown to depend on the affinity of reactive diluent with the ATNR oligomer. The most compatible system (AcTNR-TMPTA resin) allowed obtaining the highest modulus material. In addition, the presence of a low  $T_g$  ( $-50$  °C) continuous rubber phase might open a perspective for applications as damping materials at low temperature. Such results suggested that the synthesis of functional oligomers from NR could serve both for a direct development of functional bio-based materials, and as a model system for the development of waste tire recycling strategies into innovative carbon neutral materials.

## ACKNOWLEDGMENTS

We are grateful for the financial support from the MATIERES project funded by the "Région de Pays de la Loire" council. We thank to D. Queveau and J. Grison for your help concerning DMTA operation and mold preparation.

## REFERENCES

1. Pappu, A.; Patil, V.; Jain, S.; Mahindrakar, A.; Haque, R.; Thakur, V. K. *Int. J. Biol. Macromol.* **2015**, *79*, 449.
2. Thakur, V. K.; Kessler, M. R. *Polymer* **2015**, *69*, 369.
3. Thakur, V. K.; Thakur, M. K. *ACS Sust. Chem. Eng.* **2014**, *2*, 2637.
4. Thakur, V. K.; Vennerberg, D.; Kessler, M. R. *ACS Appl. Mater. Interfaces* **2014**, *6*, 9349.
5. Ciesielski, A. *An Introduction to Rubber Technology*; Rapra Technology Limited, **1999**.
6. Semegen, S. T. Ed.; *Rubber-Natural in Encyclopedia of Physical Science and Technology*, AP, **2001**.
7. Rajalingam, P.; Radhakrishnan, G.; Francis, J. D. *J. Appl. Polym. Sci.* **1991**, *43*, 1385.
8. Ravindran, T.; Nayar, M. R. G.; Francis, D. J. *J. Appl. Polym. Sci.* **1991**, *42*, 325.
9. Saetung, A.; Rungvichaniwat, A.; Campistron, I.; Klinpituksa, P.; Laguerre, A.; Phinyocheep, P.; Pilard, J. F. *J. Appl. Polym. Sci.* **2010**, *117*, 1279.
10. Jellali, R.; Campistron, I.; Pasetto, P.; Laguerre, A.; Gohier, F.; Hellio, C.; Pilard, J. F.; Mouget, J. L. *Prog. Org. Coat.* **2013**, *76*, 1203.
11. Nor, H. M.; Ebdon, J. R. *Prog. Polym. Sci.* **1998**, *23*, 143.
12. Panwiriyarat, W.; Tanrattanakul, V.; Pilard, J. F.; Pasetto, P.; Khaokong, C. *J. Appl. Polym. Sci.* **2013**, *130*, 453.
13. Pillai, V. B.; Francis, D. J. *Angew. Makromol. Chem.* **1994**, *219*, 67.
14. Saetung, N.; Campistron, I.; Pascual, S.; Pilard, J. F.; Fontaine, L. *Macromolecules* **2011**, *44*, 784.
15. E. Commission, *Landfill of Waste Directive*; Council Directive 1999/31/EC. **1999**.
16. Sidhu, S.; Kasti, N.; Edwards, P.; Dellinger, B. *Chemosphere* **2001**, *42*, 499.
17. Singh, S.; Nimmo, W.; Gibbs, B. M.; Williams, P. T. *Fuel* **2009**, *88*, 2473.
18. Martínez, J. D.; Puy, N.; Murillo, R.; García, T.; Navarro, M. V.; Mastral, A. M. *Renew. Sust. Energ. Rev.* **2013**, *23*, 179.
19. Barton, N. R.; Koutsky, J. A. *Chem. Eng. News* **1974**, *52*, 21.
20. Leyden, J. J. *Rubber World* **1991**, *203*, 28.
21. Phadke, A. A.; Bhattacharya, A. K.; Chakraborty, S. K.; De, S. K. *Rub. Chem. Technol.* **1983**, *56*, 726.
22. Nicholas, P. P. US Patent 4,161,464, **1979**.
23. Kawabata, N.; Okuyama, B. I.; Yamashita, S. *J. Appl. Polym. Sci.* **1981**, *26*, 1417.
24. Myers, R. D.; Nicholson, P.; MacLeod, J. B.; Moir, M. E. US Patent 5,602,186 (**1997**).
25. Sadaka, F.; Campistron, I.; Laguerre, A.; Pilard, J. F. *Polym. Degrad. Stab.* **2012**, *97*, 816.
26. Tran, T. K. N.; Pilard, J. F.; Pasetto, P. *J. Appl. Polym. Sci.* **2015**, *132*, 41326.
27. Jellali, R.; Campistron, I.; Laguerre, A.; Pasetto, P.; Lecamp, L.; Bunel, C.; Mouget, J. L.; Pilard, J. F. *J. Appl. Polym. Sci.* **2013**, *127*, 1359.
28. Kébir, N.; Morandi, G.; Campistron, I.; Laguerre, A.; Pilard, J. F. *Polymer* **2005**, *46*, 6844.
29. Busnel, J. P. *Polymer* **1982**, *23*, 137.
30. Trathnigg, B. In *Encyclopedia of Analytical Chemistry*; John Wiley & Sons, Ltd. **2006**.
31. Zhang, X.; Bitaraf, V.; Wei, S.; Guo, Z.; Colorado, H. A. *AIChE J.* **2014**, *60*, 266.
32. Sultania, M.; Yadaw, S. B.; Rai, J. S. P.; Srivastava, D. *Mater. Sci. Eng. A* **2010**, *527*, 4560.
33. Cook, W. D.; Simon, G. P.; Burchill, P. J.; Lau, M.; Fitch, T. J. *J. Appl. Polym. Sci.* **1997**, *64*, 769.
34. Scott, T. F.; Cook, W. D.; Forsythe, J. S. *Polymer* **2002**, *43*, 5839.
35. Girolamo, M.; Urwin, J. R. *Euro. Polym. J.* **1971**, *7*, 225.